

# Green synthesis and structural characterization of selenium nanoparticles and assessment of their antimicrobial property

Nishant Srivastava<sup>1</sup> · Mausumi Mukhopadhyay<sup>1</sup>

Received: 29 August 2014 / Accepted: 30 April 2015 / Published online: 14 May 2015  
© Springer-Verlag Berlin Heidelberg 2015

**Abstract** In the present study, selenium nanoparticles were biologically synthesized by non-pathogenic, economic and easy to handle bacterium *Ralstonia eutropha*. The selenium oxo anion was reduced to selenium nanoparticles in the presence of the bacterium. The bacterium was grown aerobically in the reaction mixture. An extracellular, stable, uniform, spherical selenium nanoparticle was biosynthesized. The TEM analysis revealed that the biosynthesized selenium nanoparticles were spherical in shape with size range of 40–120 nm. XRD and SAED analysis showed that nanocrystalline selenium of pure hexagonal phase was synthesized. The formation of actinomorphic trigonal selenium nanorods was also observed. A mechanism of biosynthesis of selenium nanoparticles by *R. eutropha* was proposed. The biosynthesized selenium nanoparticles were investigated for their antimicrobial activity against potential pathogens. Selenium nanoparticles showed excellent antimicrobial activity. The 100, 100, 250 and 100 µg/ml selenium nanoparticles were found to inhibit 99 % growth of *Pseudomonas aeruginosa*, *Staphylococcus aureus*, *Escherichia coli* and *Streptococcus pyogenes*, respectively. Similarly, the 500 µg/ml of selenium nanoparticles was found to inhibit the growth of pathogenic fungi *Aspergillus clavatus*. The antimicrobial efficacy of selenium nanoparticle was comparable with commercially available antibiotic drug Ampicillin.

**Keywords** Biosynthesis · *Ralstonia eutropha* · Selenium nanoparticles · Antibacterial

## Introduction

Selenium (Se) is one of the necessary trace elements in the human body. Approximately, 40–300 µg of Se is needed daily as dietary supplements by a normal adult [1]. Se at lower concentration is essential for maintenance of proper functioning of animal and human body [2]. High concentration of selenium (such as 3200 µg or above/day) is toxic for human body and other living organisms [1, 3]. Researchers revealed that the organoselenium inhibited the bacterial growth [4]. It is found that elemental Se at nano size carries high biological activity with low toxicity [5, 6]. This exciting property of nano Se has provided its application in medical and pharmaceutical sciences [2, 7]. Recently, selenium nanoparticle (SeNPs) has shown its excellent antibacterial activity against pathogenic bacteria *Staphylococcus aureus*. Researchers are also used SeNPs for coating on polymeric medical devices to keep them infection free. The traditional antibiotics are found ineffective on several multi drug-resistant bacteria [1]. The antioxidant activity of SeNPs is also reported by researchers. The SeNPs in size range of 5–200 nm can directly scavenge free radicals in vitro in a size dependent manner [8, 9]. The property of SeNPs is not limited to biological applications only; even it has wide use in oxidation reduction reactions, catalysis, photocells, photographic exposure meters, photocopy machines and semiconductor rectifiers [10, 11].

Conventional method for nanoparticles synthesis includes physical and chemical approaches. Physical methods are highly expensive as they required high-cost

✉ Mausumi Mukhopadhyay  
mmu@ched.svnit.ac.in;  
mausumi\_mukhopadhyay@yahoo.com

<sup>1</sup> Department of Chemical Engineering, Sardar Vallabhbhai National Institute of Technology, Surat 395007, Gujarat, India

instrument setup, optimal temperature, pH, pressure [12]. Evaporation and laser ablation techniques are some of the widely used physical processes for nanoparticles synthesis [13]. In chemical synthesis, solvents, additives, reductants or a stabilizer such as ethaline, borohydride, dodecanthiolates and many more chemicals are utilized. These chemicals are environmentally unfriendly, hazardous and toxic for living organisms [12]. The overall environmental concern has influenced researchers to replace this methodology with clean, nontoxic and environment friendly, green chemistry approach. Bacteria are the organism of choice for nanoparticles synthesis [14]. It is easy to handle, a fast growth rate, efficient and economical [2]. These small creatures have the significant ability to reduce metal ions into zero valent nanoparticles. The chemical detoxification mechanism and energy-dependent ion efflux from the bacterial cell by membrane protein have been responsible for such an interesting reduction performance [15–17]. Recently, aerobic biogenesis of SeNPs has been reported by bacteria *Pantoea agglomerans*, *Zooglea ramigera*, *Pseudomonas alcaliphila*, *Bacillus subtilis*, *Bacillus cereus*, *Duganella* sp. [2, 10, 11, 18–20] etc. Se respiring bacteria *Sulfurospirillum barnesii*, *Bacillus selenitireducens* and *Selenihalanaerobacter shrifitii* are reported for biogenesis of SeNPs in anaerobic conditions [21]. Biosynthesis in aerobic condition is much easier compared to the anaerobic biogenesis. Anaerobic biogenesis is a tiresome and difficult process [20].

In the present study, an economic, facile and environment-friendly synthesis of SeNPs by the non-pathogenic, Gram-negative, facultative litho-autotrophic, soil and fresh water bacterium *Ralstonia eutropha* is reported. The bacteria in the experiment can be a promising alternative for synthesis of SeNPs. The biosynthesized SeNPs are further evaluated for antibacterial efficacy on pathogenic strains of Gram-positive bacteria *S. aureus* (MTCC-96) and *Streptococcus pyogenes* (MTCC-442) and Gram-negative bacteria *Escherichia coli* (MTCC-443), *Pseudomonas aeruginosa* (MTCC-1688). The antifungal activity of SeNPs is also investigated on *Aspergillus clavatus* (MTCC 1323). The antimicrobial potential of biosynthesized SeNPs is determined with minimum inhibition concentration (MIC) methodology.

## Materials and methods

### Materials

Lyophilized culture of *R. eutropha* (MTCC No: 2487) was obtained from MTCC, IMTECH, Chandigarh, India. Sodium selenite ( $\text{Na}_2\text{SeO}_3$ ) and bacterial growth medium nutrient broth (N-broth) and nutrient agar was procured

from Himedia laboratories, Mumbai, India. Sterilized Milli Q water (Merck Millipore, Germany) was used throughout the experiment. All other chemicals were of analytical grade.

### Bacterial growth and preparation of biomass

The lyophilized seed culture of *R. eutropha* was revived and maintained on Nutrient agar (peptic digest of animal tissue: 5 g/L, sodium chloride: 5 g/L, beef extracts: 1.5 g/L and yeast extract: 1.5 g/L and Agar: 15 g/L; pH  $7.4 \pm 0.2$ ) slant as described by MTCC guidelines. The bacterial culture from N-Agar slant was sub-cultured in 100 ml N-broth growth medium in 250 ml Erlenmeyer flask and incubated in Orbital shaking incubator (CIS 24 BL, REMI, India) for 24 h at 30 °C. After 24 h of incubation, the bacterial biomass was harvested by centrifugation at a speed of 5000 rpm (3634 g) using Centrifuge (C30BL, REMI, India) at room temperature for 10 min for further experiment. The biomass obtained by centrifugation was washed several times using sterilized Millipore water.

### Synthesis of SeNPs by bacteria

Thoroughly washed fresh *R. eutropha* biomass (2 g wet weight) was added in 100 ml aqueous  $1.5 \times 10^{-3}$  M sodium selenite solution. The reaction mixture was incubated at 30 °C for 48 h at 120 rpm. The reaction mixture was observed for any change in color and analyzed time to time in UV visible (HACH, DR 6000, USA) spectrophotometer operated at a resolution of 1 nm. After completion of reaction, the biologically synthesized SeNPs were harvested by centrifuging the reaction mixture at 12,000 rpm (20,929 g) for 10 min. The SeNPs were washed several times with Millipore water and acetone. The washing process by centrifugation and for purification was repeated several times to avoid any impurity or any biomolecules. In the control experiment, the *R. eutropha* active biomass was autoclaved (121 °C, 15lbs for 15 min, Obromax, India) and then this autoclaved biomass was inoculated to 100 ml  $1.5 \times 10^{-3}$  M sodium selenite and allowed to react in same condition as described above with active bacteria.

### Characterization of Se nanoparticles

The size and morphology of biogenic SeNPs were characterized by transmission electron microscope (TEM, Philips Holland Tecnai-20) at accelerating voltage of 200 kV at 0.27 nm point resolution. The sample for TEM analysis was prepared by dispersing nanoparticles in acetone and placing a droplet of nanoparticles on a copper grid with mesh size of 300 and diameter of 3 nm. The excess solvent was allowed to evaporate at room temperature. The

size, size distribution and zeta potential of biogenic SeNPs was measured by a dynamic light scattering (DLS) particle size analyzer (Nano ZS 90, Malvern, UK). The elemental analysis of nanoparticles was carried out by energy dispersive X-ray (EDX) analyzer associated with scanning electron microscope (SEM) (JSM-7600F, JEOL, Japan), at an accelerating voltage of 20 kV. The XRD analysis was carried out (Xpert pro, PANalytical, Holland) at a voltage of 45 kV with Cu-K $\alpha$  radiation ( $K = 1.5406 \text{ \AA}$ ) to examine the crystalline phase of synthesized nanoparticles.

### Antimicrobial activity (MIC) of biosynthesized SeNPs

The antimicrobial activity of biologically synthesized SeNPs was investigated on pathogenic microbial isolates *E. coli* (MTCC-443), *P. aeruginosa* (MTCC-1688), *S. aureus* (MTCC-96), *S. pyogenes* (MTCC-442) and *A. clavatus* (MTCC 1323) purchased from MTCC, IMTECH Chandigarh. SeNPs (vacuum dried; powder form; washed using acetone several times) in different concentration range from 10 to 300  $\mu\text{g mL}^{-1}$  were added in bacterial suspension (adjusted to  $10^8$  CFU (colony forming unit)/ml by turbidity measurement) and incubated for 24 h at 30 °C. The concentration of SeNPs with 99 % growth inhibition after 24 h of incubation at 30 °C was considered as minimum inhibition concentration (MIC). The antibacterial activity of wet biomass of *R. eutropha* was also carried out as control experiment.

## Results and discussion

### Biosynthesis of selenium nanoparticles

The reaction mixture with activated *R. eutropha* and sodium selenite was displayed a time-dependent color change during incubation of 48 h at 30 °C, as shown in the inset of Fig. 1 (inset). At the initial point of reaction, the color of reaction mixture was light yellow, which gradually changed to red with time. After 48 h of incubation, no further change in color was observed. This red color of reaction mixture was attributed to the excitation of surface plasmon vibrations of the Se nanoparticles and provided an advantageous spectroscopic signature of their formation. In control experiments, the autoclaved bacterial cells were added into medium containing sodium selenite without changing other reaction conditions. The color of the reaction mixture was unchanged, and the reduction of  $\text{SeO}_3^-$  to  $\text{Se}^0$  was due to bacteria and its biomolecules. Autoclaving killed the bacterium and degrades enzyme, and other biomolecules present and limit their participation in reduction processes [2]. The surface plasmon

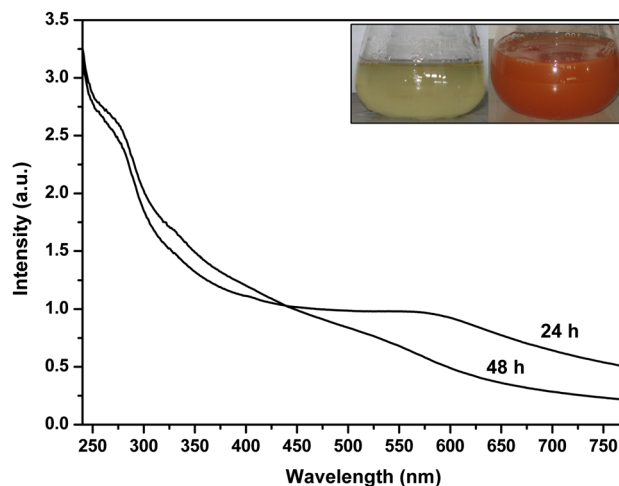
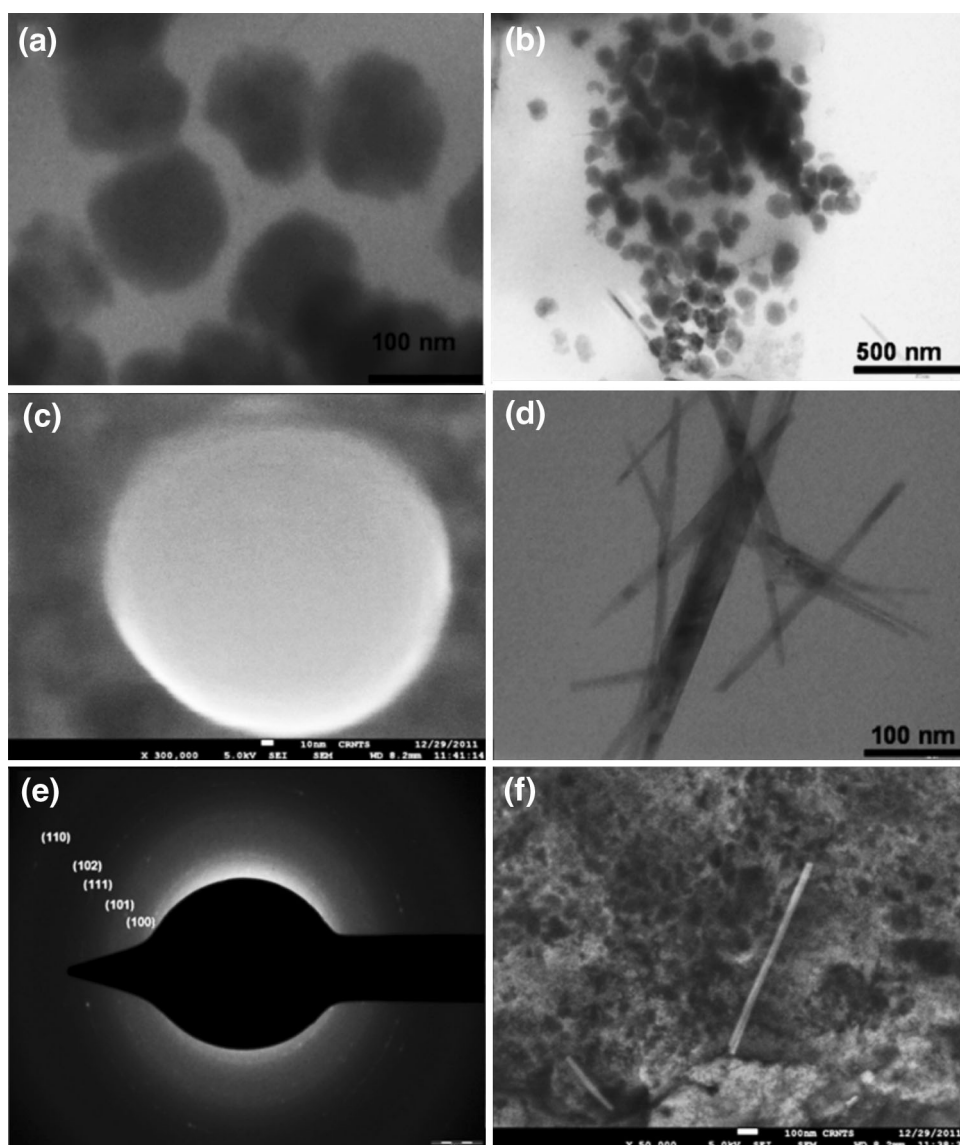


**Fig. 1** UV visible spectra of SeNPs at 24 and 48 h; Change in color of reaction mixture (initially light yellowish; Red color shows formation of SeNPs) with respect to time (Inset)

vibrations of SeNPs were also confirmed by UV–visible spectra (Fig. 1). UV–visible spectra showed the broad peak at 270 nm which confirms the formation of SeNPs. The UV spectra centered between 200 and 300 nm was due to the formation and surface plasmon vibration of SeNPs [22, 23]. The broadness of peak also revealed that the synthesized particles were polydisperse [24]. The intensity of peak increased with respect to time. There was no further significant increase in peak intensity observed after 48 h of reaction. The peak intensity was increased with time due to the reduction of  $\text{SeO}_3^{2-}$  to  $\text{Se}^0$ . There was no further increase in peak after 48 h, which depicts maximum reduction of  $\text{SeO}_3^{2-}$  to  $\text{Se}^0$ .

Figure 2 shows the electron microscopic images of SeNPs. Figure 2a and b revealed that the SeNPs were properly dispersed and spherical in shape with a diameter of 40–120 nm. Figure 2c from SEM also showed a well form of a spherical Se nanoparticle at a resolution of 10 nm scale. Formation of some actinomorphic Se nanorods was also observed in TEM and SEM analysis (Fig. 2d, f). These actinomorphic Se nanorods were also known as trigonal Se (t-Se). The formation of t-Se nanorods was due to higher free energy of SeNPs. These small SeNPs acts as a seed, which by depositing on the surface of t-Se to facilitate uniform growth of t-Se nanorods. The formation of t-Se nanorods indicated that Se nanoparticles were generated by *R. eutropha* and extended with ageing. The transformation process of small Se nanoparticles into large one was in agreement with the typical Ostwald ripening process. SAED patterns shown in Fig. 2e revealed the formation of diffraction rings, which was attributed to the (100), (101), (111), (102) and (110) reflections of nanocrystalline, hexagonal phase.

**Fig. 2** TEM and SEM micrographs of SeNPs at 100 nm scale selenium nanospheres (a) and at 500 nm scale selenium nanospheres (b), SEM image of spherical SeNPs, scale at 10 nm (c), TEM image of trigonal selenium nanorods, scale at 100 nm (d), SAED pattern shows SeNPs are hexagonal crystalline (e), and SEM image of single t-Se nanorods, scale at 100 nm (f)



The distribution of size (percentage wise) of biosynthesized selenium nanoparticles was shown in Fig. 3. The TEM image also revealed that the particles were well dispersed and uniform in shape.

The DLS analysis in Fig. 4a of colloidal solution of SeNPs showed that biosynthesized particles were in the size range of 43–121 nm with average size of 70.9 nm. The frequency distribution from the histogram showed that maximum synthesized particles were below 100 nm. The poly dispersity index (PDI) was 0.403. Lower the PDI, the lesser the aggregation of particles. The DLS results were also in agreement with TEM results. The size measured by DLS was larger than the size measured by TEM micrographs. The DLS analysis measured the hydrodynamic diameter. The corresponding zeta potential of  $-7.7$  mV observed as shown in Fig. 4b. The magnitude of zeta

potential was used to anticipate the stability of nanoparticles in colloidal solution. The zeta potential of the biosynthesized SeNPs indicated were relatively negative charged in nature. The biosynthesized nanoparticles were stable in colloidal solution to a certain extent.

The biologically synthesized Se nanoparticles formation was analyzed by EDS measurements (Fig. 5). The presence of strong peak at 1.5 keV was characteristics of Se. The presence of Se peak confirmed that the SeNPs entirely composed of Se. Some signals of Cu, Cl, P, Si and Na observed, which were associated with grid impurity used for SEM–EDS analysis. The C, P and O signals originated from biomolecules, e.g., enzymes, proteins or bacterium biomaterial either capped or present near the biologically synthesized nanoparticles. The Cu and C signals also observed this due to the presence of these elements on the SEM sample grid.

In Fig. 6, XRD analysis of biosynthesized SeNPs showed a clear, sharp Bragg reflection. The Bragg reflection peaks at  $2\theta = 23.6, 29.9, 41.4, 43.8, 45.4, 51.8, 55.9, 61.8, 65.3$  and  $68.3$  were attributed to the (100), (101),

(110), (102), (111), (201), (003), (202), (210) and (211) reflections of the pure hexagonal phase of Se crystal. The lattice parameters were  $a = 4.366 \text{ \AA}$  and  $c = 4.9536 \text{ \AA}$  (JCPDS 06-0362). The presence of sharp Bragg's reflection was in agreement with SAED pattern. The crystalline size of biosynthesized nanoparticles was calculated by Scherrer's equation:  $D = k\lambda/\beta\cos\theta$  [12, 13], where:  $\lambda$ : X-ray wavelength of  $K\alpha$ ,  $1.54 \text{ \AA}$ ,  $\theta$ : Bragg angle,  $\beta$ : half maximum in radians and  $k$ : unknown shape factor. The average crystalline size of biosynthesized Se nanoparticles obtained by Scherrer's equation was  $79 \text{ nm}$ . The *R. eutropha* mediated biologically synthesized SeNPs were crystalline and highly stable for more than 6–8 months (According to DLS analysis).

In the present study, the process used for nanoparticles synthesis is natural and microorganism driven. These microorganisms can be obtained from the environment by using simple isolation techniques. The materials required for synthesis of nanoparticles using microorganism are economical compared to the other processes. The downstream processing and purification of nanoparticle are very economical in this case. The instrument required for downstream process is the high speed centrifuge only. The

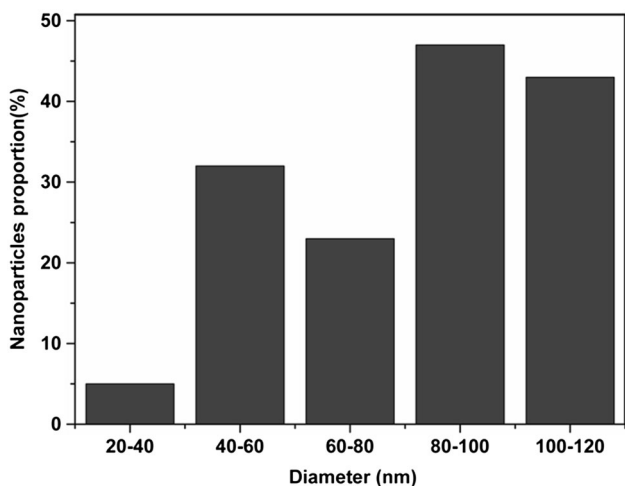


**Fig. 3** Percentage wise size distribution of SeNPs according to TEM images

**Fig. 4** DLS analysis of biosynthesized SeNPs; Size: 43–121 nm; Average size: 70.9 nm (a) and zeta potential measurement (b)

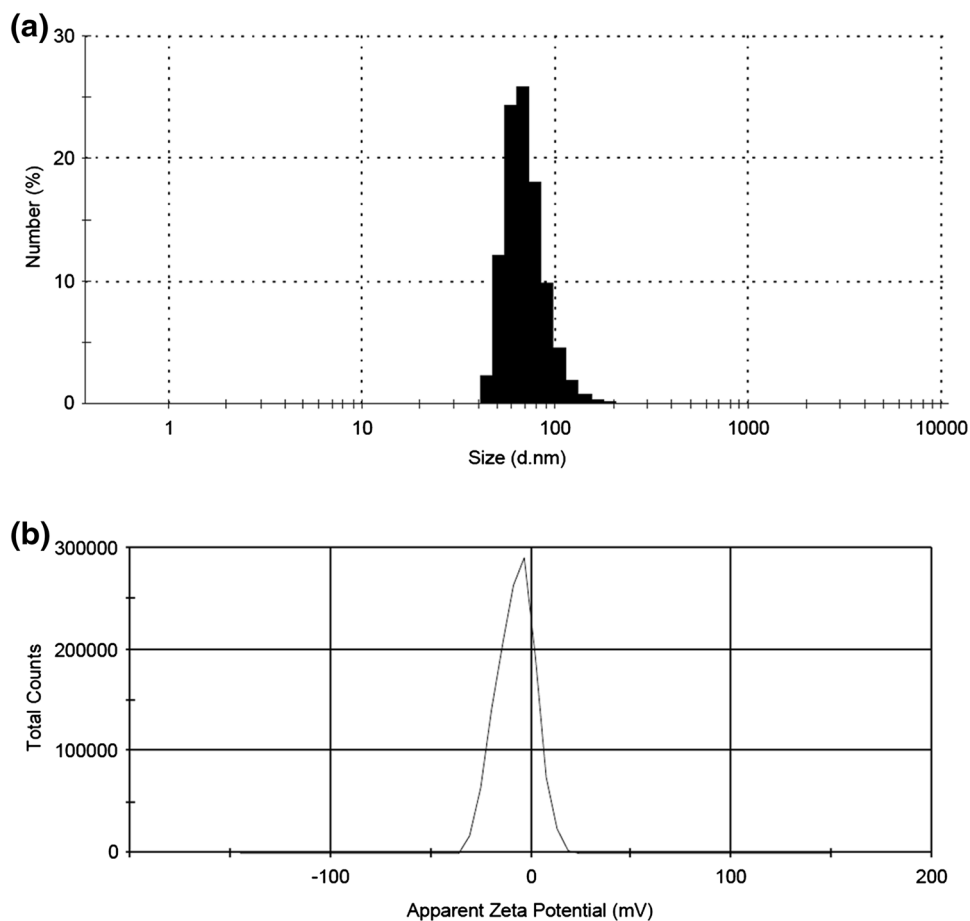


**Fig. 5** EDX pattern of biosynthesized SeNPs

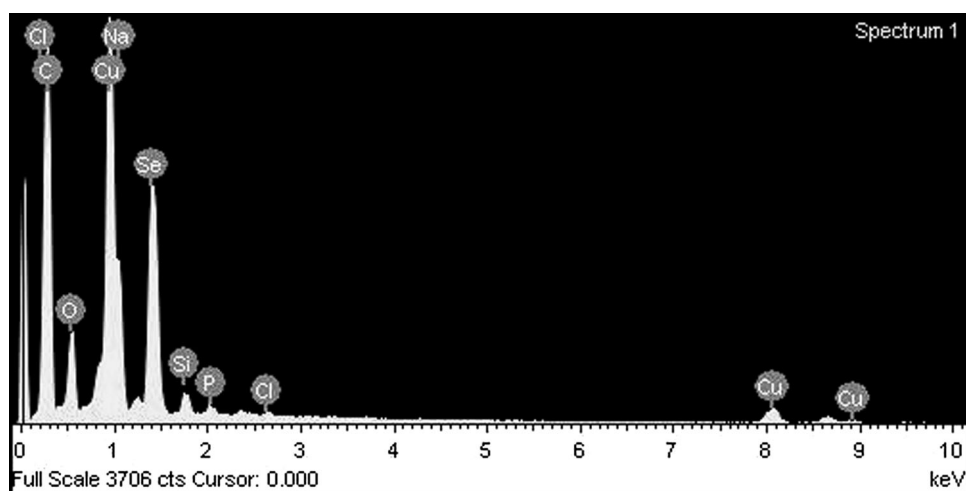
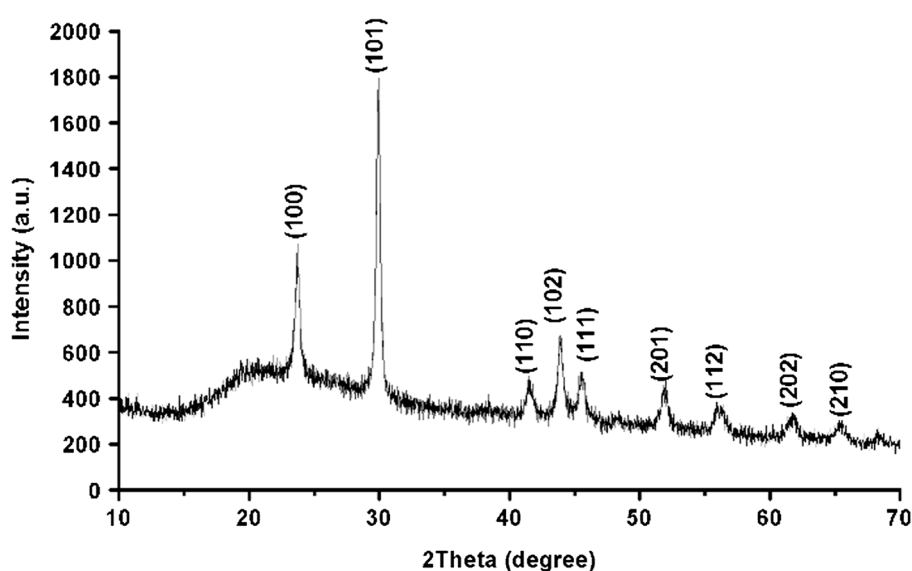


**Fig. 6** XRD of biosynthesized SeNPs by bacterium *R. eutropha*



operating cost of instruments used in the biological synthesis process is much less than instruments used in chemical or physical processes [10, 11, 17, 25, 26].

#### Antimicrobial activity (MIC) of biosynthesized SeNPs

The anti-microbial activity of SeNPs was carried out on four pathogenic bacterial strains, *E. coli*, *P. aeruginosa*, *S. aureus* and *S. pyogenes* and one fungal strain *A. clavatus*. Antibacterial drug, Ampicillin and antifungal drug, Greseofulvin were used as positive control. The self-aggregation concentration method was carried out to measure the antimicrobial activity of SeNPs. MIC was described as the amount of antimicrobial agents which inhibits 99 % microbial growth. As shown in Fig. 7, MIC of all the four potent pathogens were 125, 100, 100 and 250  $\mu\text{g/ml}$

of biosynthesized SeNPs which were found to inhibit 99 % growth of *P. aeruginosa*, *S. aureus*, *E. coli* and *S. pyogenes*, respectively. The control drug, Ampicillin showed MIC at 100, 100, 250 and 100  $\mu\text{g/ml}$  to inhibit 99 % growth of *P. aeruginosa*, *S. aureus*, *E. coli* and *S. pyogenes*, respectively. The MIC value of SeNPs showed its excellent antibacterial property. MIC of SeNPs compared to Ampicillin MIC showed better results.

In case of *S. aureus*, the MIC of SeNPs was found to be far better compared to MIC of traditional antibacterial drug, Ampicillin. SeNPs also showed a potent effect on fungi *A. clavatus*. The MIC of 500  $\mu\text{g/ml}$  was obtained for *A. clavatus* compared to MIC 100  $\mu\text{g/ml}$  of standard anti-fungal drug, Greseofulvin. The results showed that SeNPs at specific concentration inhibited the microbial growth. In control experiment, the effect of biomass also showed insignificant effects on pathogenic bacteria and fungi. The *R.*

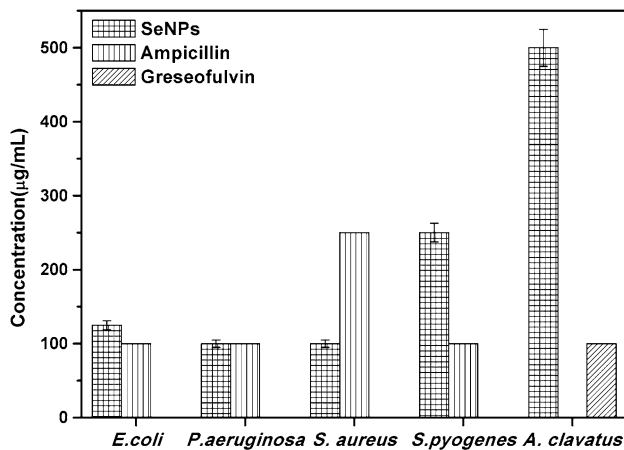


**Fig. 7** Graphical representation of MIC of SeNPs against the pathogenic bacteria *Pseudomonas aeruginosa*, *Staphylococcus aureus*, *Escherichia coli*, *Streptococcus pyogenes* and Fungi *Aspergillus clavatus*; effect of Ampicillin and Greseofulvin also shown for comparison purpose

*eutropha* biomass fails in controlling the growth of pathogenic microorganisms in the present study. The control experiment also suggested that the biomolecules, if any, present on the SeNPs surface plays a negligible role in antimicrobial activity. Up to 1 mg/L sodium selenite showed no effect on culture growth [27].

## Conclusions

*R. eutropha* mediated economical, nonhazardous, green methodology for the biosynthesis of SeNPs is reported. The bacterium found to be potent for the biosynthesis of SeNPs. Biosynthesized SeNPs are spherical in shape with size ranges between 40 and 120 nm. m-Se is dissociated in solution and precipitated out as t-Se, which further grow into actinomorphic t-Se nanorods. XRD and SAED analysis reveals that SeNPs are hexagonal crystalline. The mechanism of selenite reduction into SeNPs is also investigated. Proteins and biomolecules excreted from *R. eutropha* are believed to be responsible for the formation of SeNPs and t-Se nanorods. Proteins and other biomolecules may play a role in long-term stability of SeNPs. The biosynthesized SeNPs are used for antimicrobial evaluation on pathogenic microorganisms. The SeNPs shows exciting antimicrobial property against pathogenic strains.

**Acknowledgments** The authors like to acknowledge SAIF (Sophisticated Analytical Instrumentation Facility) and Department of Metallurgical Engineering and Material Science IITB (Indian Institute of Technology Bombay), Mumbai for providing their help in characterization of the samples.

## References

- Phong AT, Thomas JW (2013) Antimicrobial selenium nanoparticle coatings on polymeric medical devices. *Nanotechnology* 24:155101
- Srivastava N, Mukhopadhyay M (2013) Biosynthesis and structural characterization of selenium nanoparticles mediated by *Zooglea ramigera*. *Powder Technol* 244:26–29
- Navarro-Alarcon M, Cabrera-Vique C (2008) Selenium in food and the human body: a review. *Sci Total Environ* 400:115–141
- Ratushnaya EV, Kirova YI, Suchkov MA, Drevko BI, Borodulin VB (2002) Synthesis and antibacterial activity of organoselenium compounds. *Pharm Chem J* 36:652–653
- Wang H, Zhang J, Yu H (2007) Elemental selenium at nano size possesses lower toxicity without compromising the fundamental effect on selenoenzymes: comparison with selenomethionine in mice. *Free Radical Biol Med* 42:1524–1533
- Xia Y-Y (2007) Synthesis of selenium nanoparticles in the presence of silk fibroin. *Mater Lett* 61:4321–4324
- Li Q, Chen T, Yang F, Liu J, Zheng W (2010) Facile and controllable one-step fabrication of selenium nanoparticles assisted by l-cysteine. *Mater Lett* 64:614–617
- Peng D, Zhang J, Liu Q, Taylor EW (2007) Size effect of elemental selenium nanoparticles (Nano-Se) at supranutritional levels on selenium accumulation and glutathione S-transferase activity. *J Inorg Biochem* 101:1457–1463
- Prasad KS, Patel H, Patel T, Patel K, Selvaraj K (2013) Biosynthesis of Se nanoparticles and its effect on UV-induced DNA damage. *Colloids Surf B* 103:261–266
- Zhang W, Chen Z, Liu H, Zhang L, Gao P, Li D (2011) Biosynthesis and structural characteristics of selenium nanoparticles by *Pseudomonas alcaliphila*. *Colloids Surf B* 88:196–201
- Wang T, Yang L, Zhang B, Liu J (2010) Extracellular biosynthesis and transformation of selenium nanoparticles and application in H<sub>2</sub>O<sub>2</sub> biosensor. *Colloids Surf B* 80:94–102
- Singh M, Kumar M, Kalaivani R, Manikandan S, Kumaraguru AK (2013) Metallic silver nanoparticle: a therapeutic agent in combination with antifungal drug against human fungal pathogen. *Bioprocess Biosyst Eng* 36:407–415
- Bali R, Harris AT (2010) Biogenic synthesis of Au nanoparticles using vascular plants. *Ind Eng Chem Res* 49:12762–12772
- Srivastava N, Mukhopadhyay M (2014) Biosynthesis and characterization of gold nanoparticles using *zooglea ramigera* and assessment of its antibacterial property. *J Cluster Sci*. doi:10.1007/s10876-014-0726-0
- Bruins MR, Kapil S, Oehme FW (2000) Microbial resistance to metals in the environment. *Ecotoxicol Environ Saf* 45:198–207
- Srivastava S, Constanti M (2012) Room temperature biogenic synthesis of multiple nanoparticles (Ag, Pd, Fe, Rh, Ni, Ru, Pt Co, and Li) by *Pseudomonas aeruginosa* SM1. *J Nanopart Res* 14:1–10
- Srivastava N, Mukhopadhyay M (2014) Biosynthesis of SnO<sub>2</sub> nanoparticles using bacterium *Erwinia herbicola* and its photocatalytic activity for degradation of dyes. *Ind Eng Chem Res* 53:13971–13979
- Torres SK, Campos VL, León CG, Rodríguez-Llamazares SM, Rojas SM, González M, Smith C, Mondaca MA (2012) Biosynthesis of selenium nanoparticles by *Pantoea agglomerans* and their antioxidant activity. *J Nanopart Res* 14:1–9
- Bajaj M, Schmidt S, Winter J (2012) Formation of Se (0) Nanoparticles by *Duganella* sp. and *Agrobacterium* sp. isolated from Se-laden soil of North-East Punjab, India. *Microb Cell Fact* 11:1–14

20. Dhanjal S, Cameotra S (2010) Aerobic biogenesis of selenium nanospheres by *Bacillus cereus* isolated from coalmine soil. *Microb Cell Fact* 9:1–11
21. Oremland RS, Herbel MJ, Blum JS, Bevrige TJ, Ajayan PM, Sutto T, Elli AV, Curran S (2004) Structural and spectral features of selenium nanospheres produced by Se-respiring bacteria. *Appl Environ Microbiol* 70:52–60
22. Mishra RR, Prajapati S, Das J, Dangar TK, Das N, Thatoi H (2011) Reduction of selenite to red elemental selenium by moderately halotolerant *Bacillus megaterium* strains isolated from Bhitarkanika mangrove soil and characterization of reduced product. *Chemosphere* 84:1231–1237
23. Yang LB, Shen YH, Xie AJ, Liang JJ, Zhang BC (2008) Synthesis of Se nanoparticles by using TSA ion and its photocatalytic application for decolorization of congo red under UV irradiation. *Mater Res Bull* 43:572–582
24. Reddy V, Torati RS, Oh S, Kim C (2012) Biosynthesis of gold nanoparticles assisted by *Sapindus mukorossi* Gaertn. Fruit Pericarp and their catalytic application for the reduction of p-Nitroaniline. *Ind Eng Chem Res* 52:556–564
25. Srivastava N, Mukhopadhyay M (2015) Biosynthesis and structural characterization of selenium nanoparticles using *Gliocladium roseum*. *J Cluster Sci*. doi:10.1007/s10876-014-0833-y
26. Dwivedi S, AlKhedhairy AA, Ahamed M, Musarrat J (2013) Biomimetic synthesis of selenium nanospheres by bacterial strain JS-11 and its role as a biosensor for nanotoxicity assessment: a novel Se-bioassay. *PLoS One* 8:e57404
27. Araújo ILC, Afton S, Wrobel K, Caruso JA, Corona JFG, Wrobel K (2008) Study on the protective role of selenium against cadmium toxicity in lactic acid bacteria: an advanced application of ICP-MS. *J Hazard Mater* 153:1157–1164